3320 *Inorg. Chem.* **2010**, *49*, 3320–3328
DOI: 10.1021/ic9023037

Inorganic Chemistry
Article

Photoelectrochemical Behavior of Sensitized TiO_2 Photoanodes in an Aqueous Environment: Application to Hydrogen Production

Stefano Caramori,*,† Vito Cristino,† Roberto Argazzi,‡ Laura Meda,§ and Carlo A. Bignozzi*,†

†*Dipartimento di Chimica, Università di Ferrara, Via Luigi Borsari 46, 44121 Ferrara, Italy,* ‡*ISOF-CNR, c/o Dipartimento di Chimica, Università di Ferrara, Via Luigi Borsari 46, 44121 Ferrara, Italy, and* §*ENI Centro Ricerche per le Energie Non Convenzionali, Via Fauser 4, 28100 Novara, Italy*

Received November 20, 2009

The use of TiO_2 photoanodes sensitized with ruthenium(II) polypyridine complexes bearing phosphonic acid anchoring groups has been investigated in the context of photoinduced hydrogen generation. The photoanodes sustained 240 h of irradiation without undergoing appreciable hydrolysis and decomposition in an aqueous environment at pH 3. While the use of organic sacrificial donors, like ascorbic acid, considerably enhanced the photoanodic response, the exploitation of iodide was more problematic because the adsorption of photogenerated I_3^- from aqueous media favored charge recombination with conduction band electrons, thus limiting the efficiency of the photoelectrosynthetic device. However, experiments performed in a three-compartment cell, where the photolectrode was in contact with an organic solvent, showed a remarkable photocurrent, with an electrolysis yield close to 87%.

Introduction

The use of sunlight to drive thermodynamically unfavorable reactions is the primary goal of any artificial photochemical system aimed to produce electricity or valuable materials such as fuels.

The growing demand of a sustainable and renewable alternative to fossil fuels has aroused interest in photodriven hydrogen production on semiconductor substrates.

A semiconductor with a band gap higher than 1.23 eV would be required to photogenerate electron−hole pairs with sufficient driving force to carry out the two redox reactions for water splitting:

$$4H_2O + 4e^- \rightarrow 2H_2 + 4OH^-$$

$$4OH^- \rightarrow O_2 + 4e^- + 2H_2O$$

These reactions are multi-electron-transfer processes that can efficiently occur on the surface of a semiconductor provided that (a) the band edges match the redox potentials for water reduction and oxidation, (b) the charge-transfer processes at the interface are fast, and (c) the stability requirements under irradiation are met.

The simplest method to use sunlight to produce hydrogen and oxygen from water consists of the direct electrolysis of an aqueous solution by means of a solid-state photovoltaic device (e.g., silicon solar cells appropriately connected in series to reach the required overpotential for water electrolysis); however, the high cost of solar-generated power, ca. \$4/Wp,[1] limits the feasibility of this approach. An interesting alternative is to integrate the power-generating module and the electrolyzer in a single device, simplifying the construction and reducing the size and cost. This implies that the semiconductor electrode has to be immersed in solution and be resistant to photochemical degradation. A device of this type, making use of a multijunction semiconductor electrode, has been shown to reach 12.4% efficiency with a 20 h lifetime.[2]

Systems based on the semiconductor oxide/liquid electrolyte interface[3−6] have been studied for 3 decades starting from the pioneering work of Fujishima and Honda in 1972 on single-crystal TiO_2 electrodes.[7] The main reasons for using wide-band-gap oxide semiconductors, such as TiO_2, $SrTiO_3$, ZnO, SnO_2, and WO_3, for photoelectrochemical water splitting are related to their chemical inertness in most environments, their ease of fabrication through sol−gel procedures, and their low cost. However, band-gap values of nearly 3 eV or higher means that these materials do not meet the fundamental requisite of photon absorption in the visible spectrum;

*To whom correspondence should be addressed. E-mail: (S.C.), g4s@unife.it (C.A.B.).

(1) Eisenberg, R.; Nocera, G. D. *Inorg. Chem.* **2005**, *44*, 6799–6801.
(2) Khaselev, O.; Turner, J. A. *Science* **1998**, 425–427.
(3) Nozik, A. J. *Appl. Phys. Lett.* **1976**, *29*, 150.
(4) Nozik, A. J.; Fornarini, L.; Parkinson, B. A. *J. Phys. Chem.* **1984**, *88*, 3238–3243.
(5) Tan, M. X.; Laibnis, P. M.; Nguyen, S. T.; Kesselman, J. M.; Stanton, C. E.; Lewis, N. S. *Progress in Inorganic Chemistry*; John Wiley & Sons: New York , 1994; pp 21−144.
(6) Nozik, A. J.; Memming, R. J. *J. Phys. Chem.* **1996**, *100*, 13061.
(7) Fujishima, A.; Honda, K. *Naure* **1972**, *238*, 37.

Published on Web 03/08/2010

Scheme 1

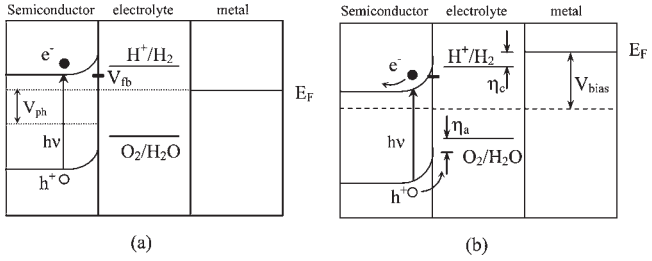

moreover, the problem encountered with colored oxides, such as Fe_2O_3 and WO_3, is that the conduction band edge is too low in energy to allow for hydrogen generation at a useful rate, and an external positive bias must be applied.[8−10]

The simplest configuration (Scheme 1) involves a semiconductor/electrolyte junction electrically connected with a metal electrode: when the semiconductor is irradiated with photons of energy corresponding to the band gap, electron−hole pairs are created and the Fermi level in the semiconductor is raised toward the flat-band potential V_{fb} by an amount V_{ph}, which is the photopotential generated.

The maximum value that the Fermi level can reach in the semiconductor is the flat-band potential V_{fb}, which, in many cases, is lower with respect to the H^+/H_2 redox couple (a). This means that hydrogen evolution cannot take place at the metal electrode even at the highest irradiation intensity. For hydrogen evolution to occur, a positive bias must be applied to the semiconductor electrode. This bias, which is usually provided by an external voltage source, should also account for the necessary cathodic (η_c) and anodic (η_a) overvoltages in order to sustain the current flow (b). The use of a p-type semiconductor instead of a metal electrode can eliminate the need for an external bias, but, again, there are problems related to the choice of the p-type semiconductor in terms of the visible-light-harvesting efficiency and photoelectrochemical stability.[11]

Sensitization of wide-band-gap semiconductor oxides, like TiO_2, can offer an alternative approach to bulk semiconductors for photodriven hydrogen production. A surface-bound sensitizer, S, acts as a light-harvesting center, collecting photons in the visible region and performing a photoinduced charge injection into the semiconductor, which is merely an electron-gathering medium. The Fermi level of TiO_2 is sufficiently negative to allow for direct hydrogen evolution at a metal (usually Pt) counter electrode without the need for a relevant external bias; however, the hole, in this case located on the sensitizer, is not usually positive enough to perform direct water oxidation at any reasonable rate. As a consequence, a sacrificial electron donor with an appropriate potential has to be employed to obtain an effective S^+ reduction. This type of conceptually simple sensitized photoelectrolytic cell is schematized in Figure 1.

In principle, D^+ could compete with the reduction of H^+ at the counter electrode, thus decreasing the hydrogen yield;

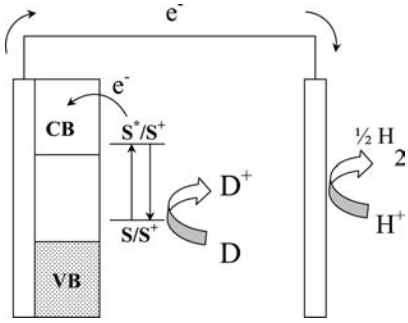

Figure 1. Working principle of a dye-sensitized photoelectrolytic device.

however, this process can be avoided, or at least minimized, by an appropriate choice of D (e.g., irreversible couples, nonelectroactive oxidized species) or simply by operating the two electrodes in separate compartments connected by a glass frit, a proton-permeable membrane, or a salt bridge. Unless sensitizers capable of performing directly an efficient water oxidation are designed,[12,13] the use of sacrificial agents, although disadvantageous, cannot be avoided. Nevertheless, it must be noted that there is a potentially large number of relatively abundant, easily oxidizable ions and organic species that could be consumed to produce hydrogen.[14−22]

Recently, Park and Bard have shown that photoinduced water splitting can be achieved with a monolithic photoelectrochemical tandem cell containing bipolar WO_3/Pt and dye-sensitized TiO_2/Pt panels, capable of vectorial electron transfer in the presence of I_2/I^- in acetonitrile.[23,24] The system represents an interesting modification of a conventional DSSC[25−27] and allows for a 1.9% hydrogen production efficiency.

In an aqueous solvent, the stability of the linkage between the molecular sensitizer and TiO_2 is crucial and requires the use of multiple anchoring groups. After a series of disappointing tests on dye molecules containing carboxylic acid functions, observed to undergo hydrolysis and desorption from the TiO_2 photoanodes, we decided to focus our studies on the series of dyes shown in Figure 2, containing phosphonic acid functions.

(8) Sartoretti, C. J.; Alexander, B. D.; Solarska, R.; Rutkowska, A. I.; Augustynski, J. *J. Phys. Chem. B* **2005**, *109*, 13685–13692.
(9) Santato, C.; Ulmann, M.; Augustynski, J. *J. Phys. Chem. B* **2001**, *105*, 936–940.
(10) Santato, C.; Ulmann, M.; Augustynski, J. *J. Am. Chem. Soc.* **2001**, *105*, 936–940.
(11) Grimes, C. A.; Varghese, O. K.; Ranjan, S. *Light, Water, Hydrogen*; Springer: New York, 2008.
(12) Alstrum-Acevedo, J. H.; Brennaman, M. K.; Meyer, T. J. *Inorg. Chem.* **2005**, *44*, 6802–6827.
(13) Youngblood, J. W.; Seung-Hyun, A. L.; Kobayashi, Y.; Ernandez Pagan, E. A.; Hoertz, P. G.; Moore, T. A.; Moore, L. A.; Gust, D.; Mallouk, T. E. *J. Am. Chem. Soc.* **2009**, *131*, 926–927.
(14) Brown, G. M.; Brunschwig, B. S.; Creutz, C.; Endicott, J. F.; Sutin, N. *J. Am. Chem. Soc.* **1979**, *101*, 1298–1300.
(15) Krishnan, C. V.; Sutin, N. *J. Am. Chem. Soc.* **1981**, *103*, 2141–2142.
(16) Graetzel, M. *Acc. Chem. Res.* **1981**, *14*, 376–384.
(17) Krishnan, C. V.; Brunschwig, B. S.; Creutz, C.; Sutin, N. *J. Am. Chem. Soc.* **1985**, *107*, 2005–2015.
(18) Arakawa, H.; Abe, R.; Sayama, K.; Domen, K. *Chem. Phys. Lett.* **2001**, *344*, 339–344.
(19) Arakawa, H.; Abe, R.; Sayama, K. *Chem. Phys. Lett.* **2002**, *362*, 441–444.
(20) Arakawa, H.; Abe, R.; Sayama, K. *Chem. Phys. Lett.* **2003**, *379*, 230–235.
(21) Dempsey, J. L.; Esswein, A. J.; Manke, D. R.; Rosenthal, J.; Soper, J. D.; Nocera, G. D. *Inorg. Chem.* **2005**, *44*, 6879–6892.
(22) Abe, S.; Sayama, K.; Arakawa, H. *J. Photochem. Photobiol. A* **2004**, *166*, 115.
(23) Park, J. H.; Bard, A. J. *Electrochem. Solid State Lett.* **2005**, *8*, G371–G375.
(24) Park, J. H.; Bard, A. J. *Electrochem. Solid State Lett.* **2006**, *9*, E5–E8.
(25) Graetzel, M. *Inorg. Chem.* **2005**, *44*, 6841–6851.
(26) Hagfeldt, A.; Graetzel, M. *Acc. Chem. Res.* **2000**, *33*, 269.
(27) O'Regan, B.; Graetzel, M. *Nature* **1991**, *353*, 737.

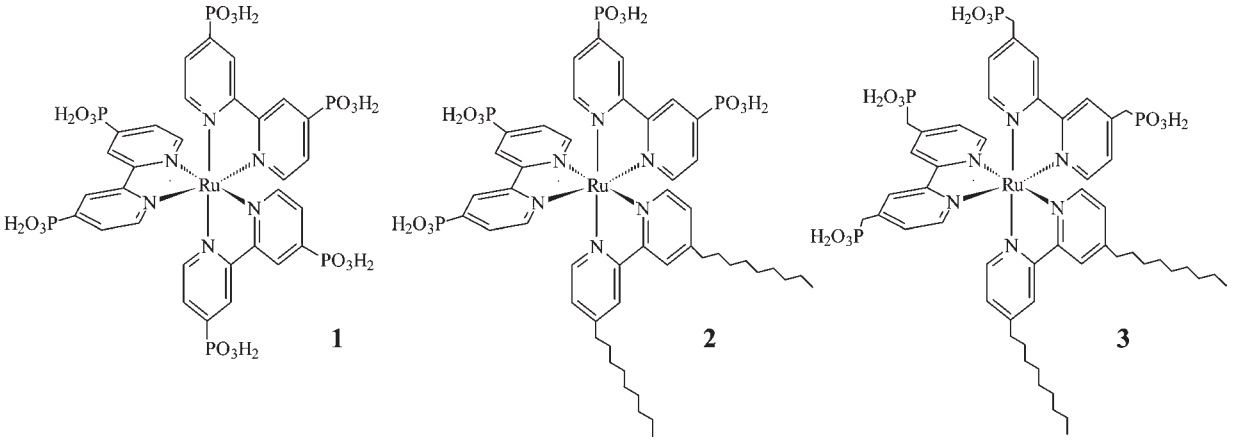

Figure 2

In this paper, we report the results of a photoelectrochemical and photophysical investigation on TiO_2 photoanodes sensitized with the molecular species **1**−**3**, which display a remarkable adsorption stability and allow for visible-light harvesting, charge injection, and hydrogen production at a Pt counter electrode in aqueous solutions containing iodide, chloride, isopropyl alcohol, or ascorbic acid as sacrificial donors.

Experimental Section

Materials. Sodium iodide (NaI), sodium chloride (NaCl), sodium sulfate (Na_2SO_4), titanium tetraisopropoxide [Ti(ip)$_4$], titanium tetrachloride ($TiCl_4$), 4,4′-dinonyl-2,2′-bipyridine (dnbpy), dichloro-*p*-cymeneruthenium(II) dimer, spectroscopic-grade acetonitrile (ACN), dimethylformamide (DMF), ascorbic acid, isopropyl alcohol, formic acid, and lithium chloride were from Aldrich and Fluka. Ruthenium trichloride ($RuCl_3$) was from Alfa Aesar. The phosphonic ligand 2,2′-bipyridine-4,4′-dimethylenediphosphonic ethyl ester [bpy-$(CH_2PO_3(CH_2CH_3)_2)_2$] was available from a previous work. The 2,2′-bipyridine-4,4′ ethyl ester [bpy$(PO_3(CH_2CH_3)_2)_2$] ligand was purchased from Hetcat. Sephadex LH 20 was provided by GE Healthcare Biosciencies. Conductive glass sheets (fluorine−tin oxide, FTO; 8 Ω/□) were purchased from Hartford Glass. Titanium dioxide (TiO_2) preparation, $TiCl_4$ treatment, and electrode fabrication were performed according to previously published procedures.[28] Unless otherwise stated, all chemicals were used as received.

Synthesis. $[\mathbf{Ru(bpy(PO_3H_2)_2)_3}]^{2+}$ **(1).** $RuCl_3 \cdot 3H_2O$, dissolved in DMF, was refluxed under nitrogen in the presence of a 3-fold molar excess of bpy$(CH_2PO_3(CH_2CH_3)_2)_2$. The progress of the reaction was monitored by thin-layer chromatography (TLC) on silica gel (methanol as the eluant) and UV−vis spectroscopy. After completion of the reaction, testified by the disappearance of the purple spot corresponding to the intermediate [Ru(bpy$(PO_3H_2)_2)_2Cl_2$], the solvent was evaporated under reduced pressure and the crude product was dissolved in water and purified by size-exclusion chromatography (LH 20/water). The desired product, corresponding to an intense orange band, was collected and refluxed in 6 M HCl for 12 h to obtain complete hydrolysis of the ethyl ester groups, which were found partially hydrolyzed during the DMF stage.

Subsequent purification on an LH 20 column afforded the desired product with a good degree of purity.

Anal. Calcd for $Ru(C_{30}H_{30}Cl_2N_6O_{18}P_6)$: H, 2.7; C, 32.16; N, 7.5. Found: H, 2.67; C, 32.10; N, 7.48.

^{1}H NMR (300 MHz, D_2O): δ 8.5 (d, 6H), 7.6 (m, 6H), 7.36 (m, 6H).

ESI MS: m/z 524 (M^{2+}).

$\mathbf{[Ru(dnbpy)(bpy(PO_3H_2)_2)]^{2+}}$ **(2).** A 2.76×10^{-2} g (4.5×10^{-5} mol) amount of a dichloro-*p*-cymeneruthenium dimer dissolved in ca. 10 mL of DMF was reacted, under nitrogen, with 3.68×10^{-2} g (9×10^{-5} mol) of dnbpy at 70 °C for 5 h. After this time, 8.2×10^{-2} g (18×10^{-5} mol) of (bpy$(PO_3(CH_2CH_3)_2)_2$) was added, and the resulting solution was refluxed for a further 4 h. The progress of the reaction was monitored by TLC and UV−vis spectroscopy. After completion of the reaction, the solvent was evaporated under reduced pressure and the crude product was purified by size-exclusion chromatography (LH 20/water). The desired product was collected and refluxed in 6 M HCl for 15 h to obtain complete hydrolysis of the ethyl ester groups.

Subsequent purification on an LH 20 column afforded the desired product with a good degree of purity.

Anal. Calcd for $Ru(C_{48}H_{54}Cl_2N_6O_{12}P_4)$: H, 4.53; C, 47.93; N, 6.99. Found: H, 4.50; C, 47.89; N, 7.01.

^{1}H NMR (300 MHz, CD_3OD): δ 8.95 (d, 4H), 8.7 (s, 2H), 8.05 (m, 4H), 7.4 (m, 4H), 7.25 (d, 2H), 7 (d, 2H), 2.9 (br m, 4H), 2.1 (br m, 4H), 1,2 (br m, 24H), 0.9 (br m, 6H).

ESI MS: m/z 577 (M^{2+}).

$\mathbf{[Ru(dnbpy)(bpy(CH_2PO_3H_2)_2)]^{2+}}$ **(3).** This complex was prepared following the procedure described for **2**, by using the bpy$(CH_2PO_3(CH_2CH_3)_2)_2$ ligand.

Anal. Calcd for $Ru(C_{52}H_{62}Cl_2N_6O_{12}P_4)$: H, 4.96; C, 49.61; N, 6.68. Found: H, 4.92; C, 49.58; N, 6.65.

^{1}H NMR (300 MHz, D_2O): δ 8.35 (d, 4H), 8 (s, 2H), 7.75 (m, 2H), 7.4 (m, 2H), 7.2 (m, 2H), 7.5 (m, 6H), 3.7 (br m, 4H), 3.05 (br s, 4H), 2.5 (br s, 4H), 1.35 (br m, 4H), 0.95 (br m, 24H), 0.55 (br m, 6H).

ESI MS: m/z 562 (M^{2+}).

TiO_2 Sensitization. TiO_2 sensitization was carried out by immersion of the TiO_2 electrodes in a 50:50 water/methanol sensitizer solution ($\approx 10^{-4}$ M) for 12 h, in the dark, at room temperature. If needed, dye adsorption could be accelerated by moderate heating (50−60 °C). In such conditions, adsorption was completed within 3−4 h. These photoelectrodes exhibited a strong absorption in the visible region, with optical densities ≥ 1.3 in correspondence with the metal-to-ligand charge-transfer (MLCT) maximum of the dye.

Apparatus and Methods. Electrochemical characterization of the ruthenium dye sensitizers in solution and anchored to an FTO surface was carried out by cyclic voltammetry (CV) in an aqueous 1 M Na_2SO_4 supporting electrolyte. Incident photon-to-current conversion efficiency (IPCE)[29] spectra were collected

(28) Cazzanti, S.; Caramori, S.; Argazzi, R.; Elliott, C. M.; Bignozzi, C. A. *J. Am. Chem. Soc.* **2006**, *128*, 9996–9997.

(29) Nazeeruddin, M. K.; Kay, A.; Rodicio, I.; Humphry-Baker, R.; Mueller, E.; Liska, P.; Vlachopoulos, N.; Graetzel, M. *J. Am. Chem. Soc.* **1993**, *115*, 6382–6390.

Scheme 2. Experimental Setup for Photoelectrolysis Experiments with Partitioned Solvents

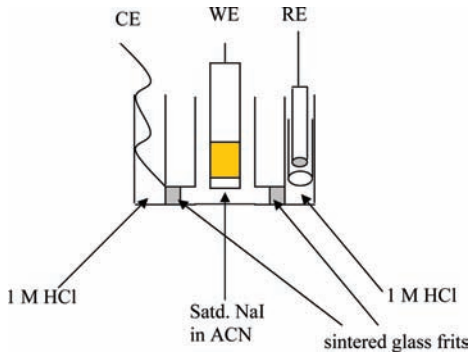

by focusing the monochromatic light generated by an Applied Photophysics monochromator (spectral bandwidth = 10 nm) onto the photoanode of a three-electrode photoelectrochemical cell (sensitized TiO_2/Pt/SCE) connected to an AMEL model 552 potentiostat. The illuminated area was 0.5 cm^2. Short-circuit photocurrents were measured with an Agilent 34401A multimeter. Incident irradiance was calculated by means of a Centronic OSD 100-7Q calibrated silicon photodiode. $J-V$ curves and photocurrent and photopotential transients were obtained under the white visible light generated by an HID lamp, filtered from its weak UV component by a 420 nm cutoff filter, by using an EcoChemie PGSTAT 30 electrochemical workstation connected to a conventional three-electrode cell. Incident white-light irradiance was measured with a Molectron Powermax 5200 power meter and set to approximately 0.1 W/cm^2.

Photoelectrochemical experiments using a three-compartment cell configuration were performed by immersion of the photoanode (working electrode) in a NaI/ACN solution while the reference and counter electrodes were immersed in a 1 M HCl aqueous solution. Each electrode compartment was separated by a glass frit, as shown in Scheme 2.

Qualitative gas chromatographic detection of hydrogen was performed with a Varian CP 4900 micro gas chromatograph equipped with a molecular sieves column and a thermal conductivity detector.

The moles of produced hydrogen were calculated by measuring the volume of hydrogen gas collected in a 1 mL graduated syringe at T = 287 K (14 °C) and at P = 1013 hPa. The electrolysis yield was calculated from the ratio between the moles of collected hydrogen and those predicted on the basis of the Faraday law.

Time-resolved spectroscopic experiments were carried out in air by using carefully rinsed and air-dried sensitized TiO_2 films (active area 4 × 1 cm) previously subjected to specific photoelectrochemical experiments (see the Supporting Information).

Conduction band electrons to dye cation recombination kinetics, observed at 450 nm (band pass ≈ 21 nm), were obtained by excitation of the sensitized TiO_2 films with the second harmonic (532 nm) of a Nd:YAG laser (fwhm = 7 ns) using the transient absorption apparatus previously described.[28] Laser pulses were attenuated with a chemical filter (aqueous $KMnO_4$, 5% T at 532 nm) and defocused with a plano concave lens to achieve pulse energies of ca. 1 mJ/cm^2/pulse. To avoid direct TiO_2 excitation, a 400 nm cutoff filter protected the sensitized TiO_2 photoelectrode sample from exposure to the UV light contained in the probe beam. Under such conditions, no sample degradation was detected over several repeated laser pulses. An interference filter oriented at 45° prevented laser stray light from reaching the detector, avoiding possible artifacts originating by direct scattered laser light detection and/or photomultiplier blinding. Decays with a satisfactory signal-to-noise ratio were usually obtained by averaging 10 laser shots.

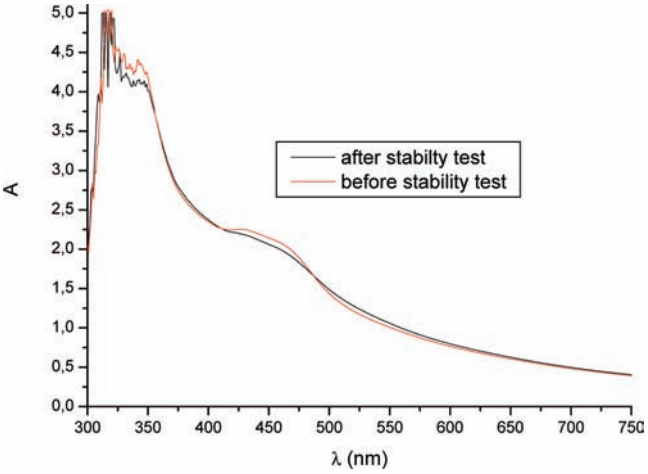

Figure 3. Absorption spectra of **1** loaded on a transparent TiO_2 photoelectrode before (red) and after (black) immersion in 0.1 M $LiClO_4$ in a 8:2 water/isopropyl alcohol electrolyte for 30 days.

Results and Discussion

The stability of the bonding between the dye sensitizer and the TiO_2 surface in an aqueous medium is crucial and requires the use of multiple anchoring groups. Thus, the phosphonic groups have been selected for their strong interaction with metal oxides because of their ability to form a tripodal linkage.[30] Our attention has been focused on the ruthenium(II) tris(bipyridine) type design with the following goals in mind: (i) reversible $Ru^{II/III}$ oxidative processes at anodic potentials ($E_{1/2} \geq 1$ V vs SCE); (ii) intense visible absorption bands ($\lambda < 600$ nm) associated with strongly reducing MLCT excited states; (iii) high photochemical stability in coordinating solvents.

All of these requirements are oriented to obtain the necessary chemical and photochemical stability for operating the photoelectrode in aqueous media for long periods without dye decomposition and to allow for charge injection into the TiO_2 conduction band while maintaining a sufficient driving force for oxidation of a potentially large number of sacrificial electron donors.

The nonyl substituents of complexes **2** and **3** have been introduced to enhance the stability against desorption phenomena thanks to the formation of an hydrophobic network originating from the interdigitated alkyl chains.[31,32] Moreover, steric hindrance of these chains contributes to the slowdown of electron recapture by an oxidized electron donor.[33]

Both the adsorption and photochemical stabilities of complexes **1**−**3** on the TiO_2 surface are remarkable and are testified, as an example, by a comparison of the absorption spectra of **1** (Figure 3) recorded before and after 1 month of continuous immersion in a 8:2 water/isopropyl alcohol mixture, during which the photoelectrode was exposed to 240 h of visible-light irradiation ($\lambda > 420$ nm, ≈0.1 W/cm^2) under short-circuit conditions.

(30) Gillaizeau-Gautier, I.; Odobel, F.; Alebbi, M.; Argazzi, R.; Costa, E.; Bignozzi, C. A.; Qu, P.; Meyer, G. J. *Inorg. Chem.* **2001**, *40*, 6073–6079.
(31) Zakeeruddin, S. M.; Nazeeruddin, M. K.; Pechy, P.; Quagliotto, P.; Barolo, C.; Viscardi, G.; Graetzel, M. *Langmuir* **2002**, *18*, 952.
(32) Wang, P.; Zakeeruddin, S. M.; Comte, P.; Charvet, R.; Humphry-Baker, R.; Graetzel, M. *J. Phys. Chem. B* **2003**, *107*, 14336–14341.
(33) Klein, C.; Nazeeruddin, M. K.; Di Censo, D.; Liska, P.; Graetzel, M. *Inorg. Chem.* **2004**, *43*, 4216–4226.

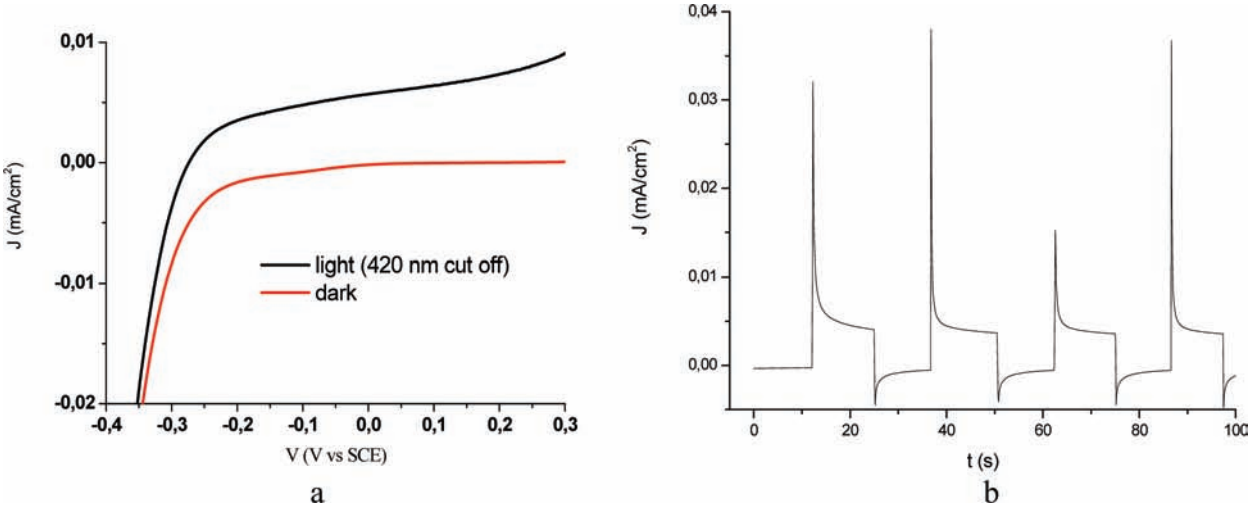

Figure 4. (a) $J-V$ curves of **1** in water/0.1 M $LiClO_4$ at pH 5 ($HClO_4$). (b) Photocurrent transients under 0 mV vs SCE potential bias.

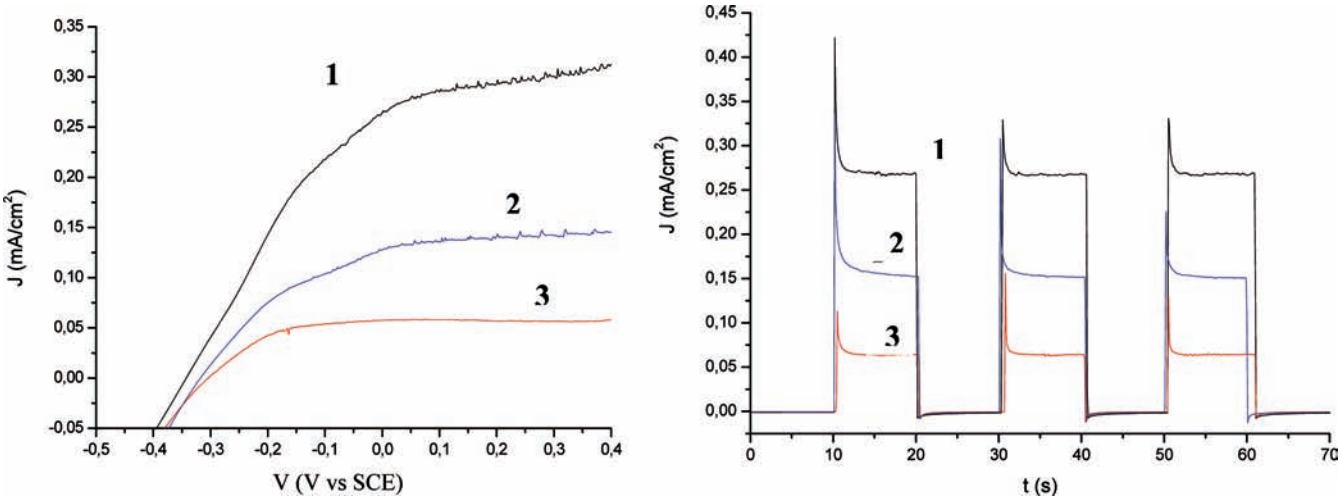

Figure 5. (a) $J-V$ curves for complexes **1**−**3** in 8:2 (v/v) water/isopropyl alcohol/0.1 M $LiClO_4$ at pH 3 ($HClO_4$). (b) Photocurrent transients under 0 mV vs SCE potential bias.

The electrolyte solution consisting of 0.1 M $LiClO_4$ in 8:2 water/isopropyl alcohol at pH 3 ($HClO_4$) was renewed on a daily basis, and the photocurrent density was observed to be substantially stable, within 250 ± 20 $\mu A/cm^2$.

The $Ru^{II/III}$ oxidation potentials of the selected dye sensitizers are decreasing in the order **1** (1.20 V vs SCE) > **2** (1.18 V vs SCE) > **3** (0.94 V vs SCE). The trend is expected on the basis of the substituents at the 4 and 4′ positions of the bipyridines: in **3**, the methylene spacers attenuate the electron-withdrawing inductive effect of the phosphonates, leading to destabilization of the metal dπ orbitals, which results in an oxidation potential evidently less positive than those of **1** and **2**, which show energetically close processes. The wave separation is in all cases on the order of 80−100 mV, without cell resistance compensation, indicating a fast electron transfer, expected in the case of redox processes involving $Ru^{II/III}$ dπ orbitals.[34]

1. Organic Sacrificial Agents. In the most favorable case (complex **1**), it was possible to observe production of a photoanodic current in the presence of plain water/0.1 M $LiClO_4$ at pH 5 ($HClO_4$). However, despite a reasonable negative free-energy difference for water oxidation (ca. 0.46 V, considering that the thermodynamic potential for oxygen evolution at pH 5 is 0.95 V vs NHE), the photocurrent was extremely small, ca. 5 $\mu A/cm^2$ (Figure 4a). Chronoamperometry under pulsed illumination (Figure 4b) revealed the presence of a fast relaxation from the initial value, reached as soon as the electrode was exposed to light, and the presence of dark cathodic features. Both characteristics are indicative of an inadequate dye regeneration efficiency, which is reflected in an interfacial hole accumulation, leading to an effective photoinjected electron to Ru^{III} recombination.[35]

The addition of 20% (v/v) isopropyl alcohol leads to a general increase of the performances, allowing for the delivery of a maximum photocurrent density of 300 $\mu A/cm^2$ in the case of **1**. The photoanodic current (Figure 5) increases in the order **3** < **2** < **1**, in agreement with the relative $Ru^{II/III}$ oxidation potentials. The photocurrent transients collected in the presence of a 0 mV vs SCE potential bias approach a more ideal rectangular shape,

(34) Balzani, V.; Juris, A. *Coord. Chem. Rev.* **1988**, *84*, 85–277.

(35) Hammett, A; Dare edwards, M. P.; Wright, R. D.; Seddon, K. R.; Goodenough, J. B. *J. Phys. Chem.* **1979**, *83*(25), 3280–3290.

although both the initial relaxation and the cathodic features are still evident. The latter are, however, barely observable, indicating that isopropyl alcohol effectively acts as an electron donor, promoting Ru^{III} reduction.[36]

Ascorbic, citric, and formic acids may represent an additional interesting class of water-soluble sacrificial electron donors. In particular, ascorbic acid has been used as an electron donor in photocatalytic hydrogen-evolving systems in a homogeneous phase, some of which involved the use of ruthenium polypyridine complexes as light-harvesting and photoreactive centers.[37] Moreover, the carboxylic function promotes their adsorption on the titania surface, increasing the probability of interaction with the dye molecules. Ascorbic acid was found to be an effective electron donor, resulting in a maximum IPCE of 24% in the 430−500 nm region, with a photoaction onset at 675 nm (Figure 6). Correspondingly, under white-light irradiation, photocurrents higher than 2 mA/cm^2 were achieved with **1** at 0 mV vs SCE and a photoanodic plateau of ca. 3 mA/cm^2 was observed under a slightly positive bias (0.2 V vs SCE; Figure 7). Hydrogen collection experiments revealed a satisfactory electrolysis yield (96.7%), which resulted in the production of 2.96×10^{-5} mol of H_2 in 2680 s.

Rectangular-shaped photocurrent transients indicate a strongly decreased electron back recombination involving Ru^{III} and a good reproducibility of the photoanodic processes. On the contrary, formic acid, which is known to be an effective hole scavenger for bare TiO_2 (upon direct band-gap excitation), was revealed to be inadequate for regenerating the sensitizer, producing a marginal improvement over the pure water/$LiClO_4$ electrolyte. This evidence is related to the exceedingly positive potential for formic acid oxidation, which could not be observed by CV at a glassy carbon electrode in water/$LiClO_4$ in the interval 0−1.2 V vs SCE; on the contrary, under the same conditions, ascorbic acid gave a clear irreversible oxidation wave with a peak at 0.36 V vs SCE.

2. Halides. The use of chlorides as sacrificial agents in either aqueous or organic media did not lead to relevant performances (Figure 9). The best results were obtained with complex **1**: in the presence of a positive bias of 0.4 V vs SCE, photocurrents of 120 ± 20 μA/cm^2 were measured. At 0 mV vs SCE, **2** and **3** produce lower photoanodic currents (ca. 60 μA/cm^2). The photocurrent transients recorded at 0 mV vs SCE (Figure 8b) indicate for all

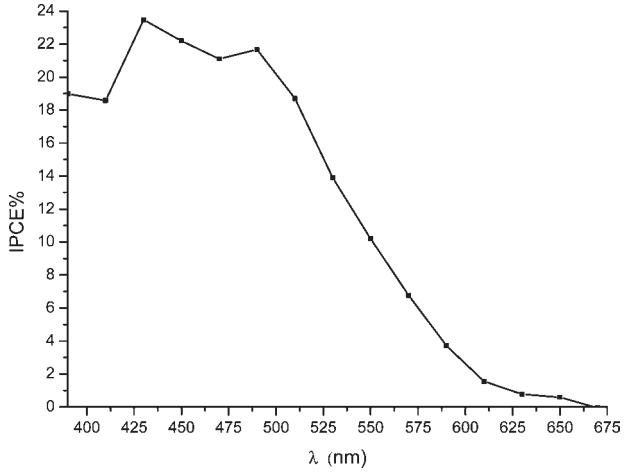

Figure 6. Photoaction spectrum of complex **1** in the presence of 1 M ascorbic acid and 0.1 M $LiClO_4$ in water. Bias: 0 mV vs SCE.

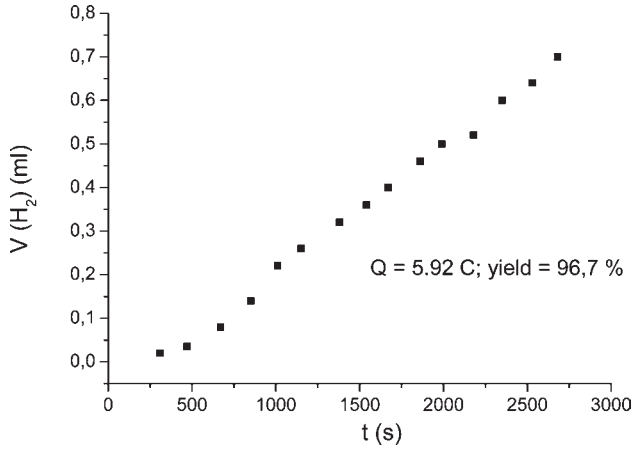

Figure 8. Volume of produced hydrogen as a function of time during photoelectrolysis employing ascorbic acid as a sacrificial electron donor.

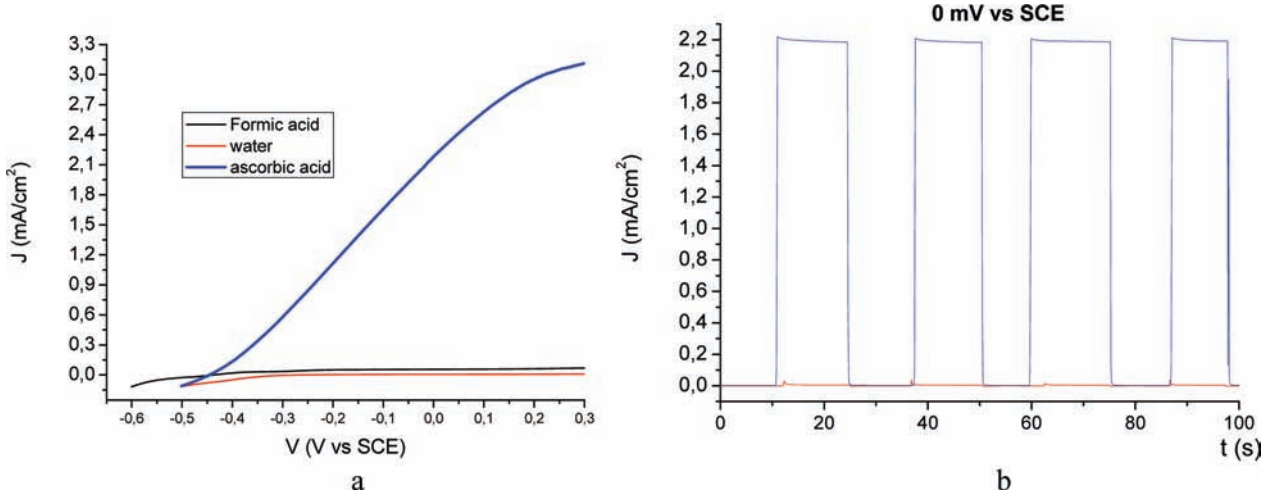

Figure 7. (a) $J-V$ curves for complex **1** in water: 1 M ascorbic acid/0.1 M $LiClO_4$ (blue); 1 M formic acid/0.1 M $LiClO_4$ (black); 0.1 M $LiClO_4$ (red). (b) Photocurrent transients under 0 mV vs SCE potential bias.

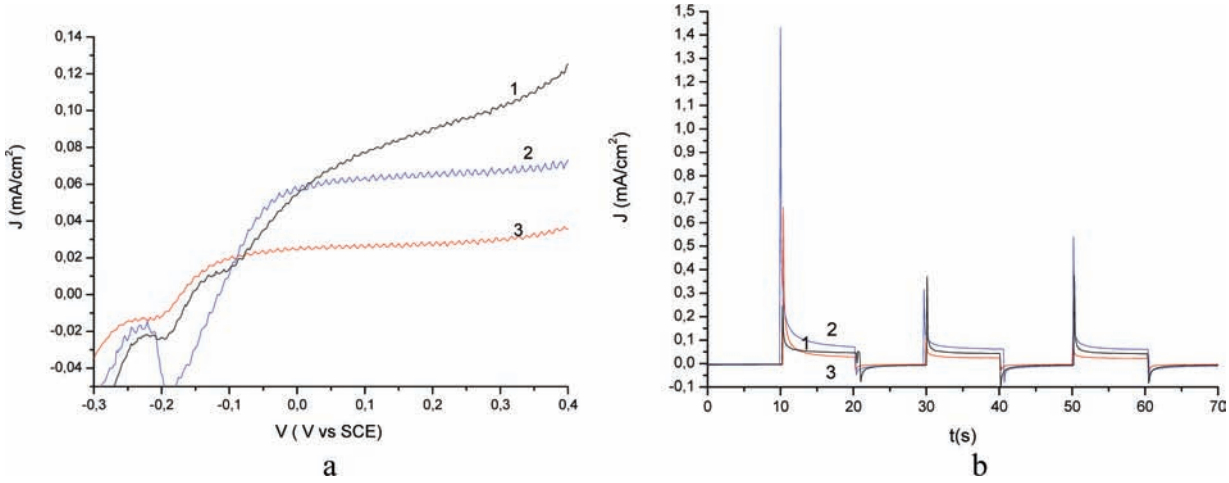

Figure 9. (a) $J-V$ curves for complexes **1**−**3** in aqueous 1 M NaCl at pH 3. (b) Photocurrent transients under 0 mV vs SCE potential bias.

complexes an inefficient Ru^{II} recovery, most probably because of the small driving force for Cl^- oxidation by Ru^{III} [$E^{0'}(Cl_2/Cl^-) = 1.1$ V vs SCE].

Iodide was expected to be a better hole scavenger because its formal oxidation potential is on the order of 0.4 V vs SCE; however, the use of aqueous iodide solutions led to instability of the photoanodic response of the sensitized anodes, and the reasons for such behavior were investigated in detail.

All complexes effectively sensitize transparent titania. As an example, complex **3** gives rise to photoelectrodes with a maximum visible absorbance of 1.5−1.7. The photoresponse in ACN in the presence of I^-/I_3^- is substantially stable with time, and the photoaction spectrum shows the usual and expected features, matching the dye absorption spectrum with a maximum IPCE on the order of 60% (Figure S1a in the Supporting Information). In aqueous media, initial maximum IPCE values of 30% (Figure S1b in the Supporting Information) were observed to decrease to maximum stationary values on the order of 5−6% in a time scale of a few seconds (Figure S1b, red line, in the Supporting Information) independent of the pH and type of iodide salt (LiI, NaI, HI, and KI). An entirely analogous behavior extends to complexes **1** and **2**.

Photocurrent transients recorded in aqueous 1 M NaI at pH 3 ($HClO_4$) under 0.1 W/cm^2 white-light irradiation confirmed the photoanodic instability: within a few seconds, the photocurrent decreases from an initial value of 5 mA/cm^2 to 0.5 mA/cm^2 without recovering to the initial value in subsequent irradiation cycles (Figure S2 in the Supporting Information).

The $J-V$ curves recorded on photoanodes sensitized with **3** under shuttered illumination (Figure 10) show, in the 0 to −300 mV interval, the expected decrease in the photoresponse, determined by a combination of increased charge recombination from progressively filled higher-lying TiO_2 states and a decreased driving force for the charge-injection process. In the −300 to −500 mV range, however, enhanced photoanodic transients are

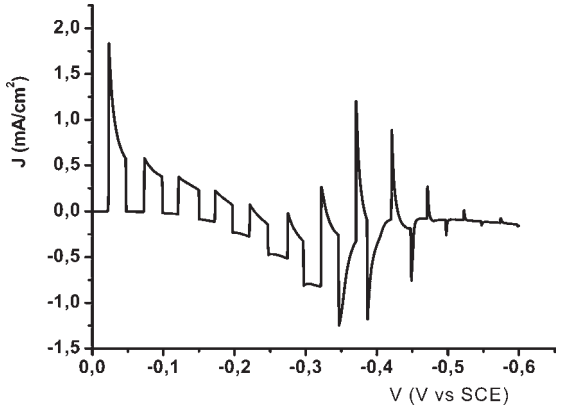

Figure 10. Photocurrent transients as a function of the applied potential for a photoanode sensitized with complex **3**. Scan speed 10 mV/s.

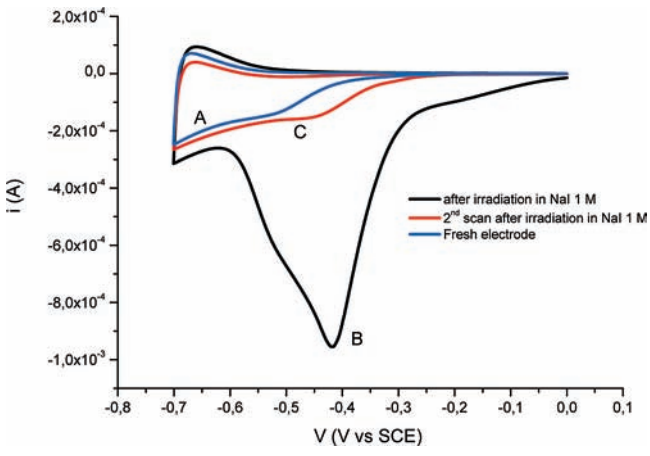

Figure 11. CV of a TiO_2 electrode sensitized with **3** in aqueous 1 M NaCl: (A) freshly prepared electrode (blue line); (B) after 60 s of irradiation in 1 M NaI and rinsing with water (black line); (C) same as that in part B, second scan. Scan speed 20 mV/s. Potentials referred to SCE.

followed by a fast decay and by sharp cathodic spikes when the light is turned off. This behavior is consistent with the presence of surface-adsorbed I_3^-: at potentials approaching I_3^- reduction, a local surface excess of I^- is produced and readily intercepted by the photooxidized sensitizer, giving rise to the sharp photoanodic transients

(36) Treadway, J. A.; Moss, J. A.; Meyer, T. J. *Inorg. Chem.* **1999**, *38*, 4386–4387.
(37) Na, Y.; Wang, M.; Pan, J.; Zhang, P.; Akermark, B.; Suin, L. *Inorg. Chem.* **2008**, *47*, 2805–2810.

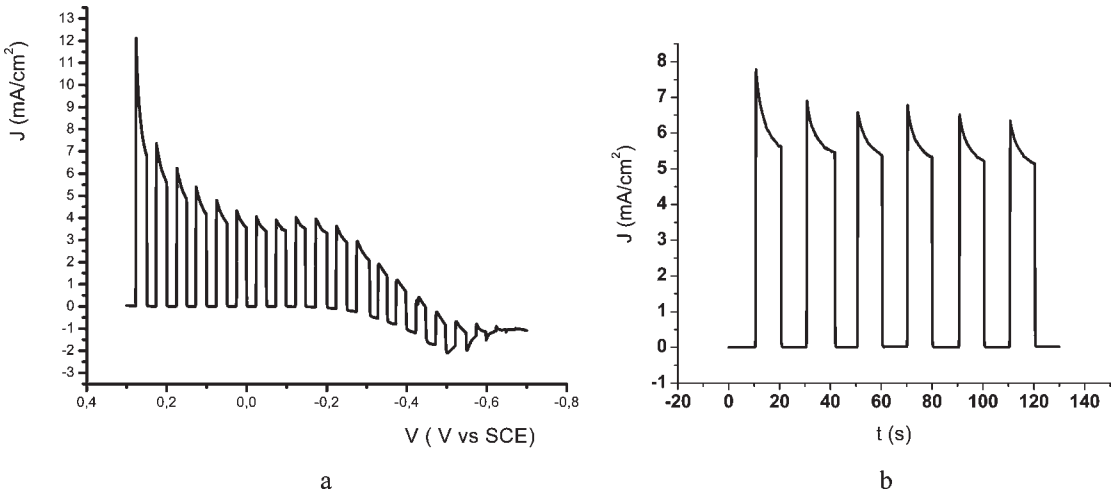

Figure 12. (a) $J-V$ shuttered curve recorded in saturated NaI in ACN using the cell arrangement of Scheme 1. Scan speed 10 mV/s. (b) Photoanodic response upon subsequent irradiation cycles at 0 mV vs SCE.

followed by cathodic features caused by efficient back recombination with I_3^-. At potentials more negative than −500 mV vs SCE, the photoanodic current is largely suppressed as the flat-band potential of the semiconductor is approached.

The hypothesis of triiodide adsorption is corroborated by CV recorded in an aqueous NaCl supporting electrolyte, by using photoanodes previously irradiated (60s) under 0 mV vs SCE potential bias in a 1 M NaI solution (Figure 11).

The CV recorded in a NaCl solution using the freshly prepared photoelectrode shows the expected reduction peak due to the $Ti^{4+} \rightarrow Ti^{3+}$ process, evident for potentials more negative than −0.5 V vs SCE. The same electrode, after irradiation in NaI, (Figure 11B) shows an intense, triangular-shaped irreversible peak, with a maximum at − 420 mV vs SCE, due to the adsorbed triiodide reduction. Triiodide is irreversibly consumed during the first scan and diffuses away from the electrodic surface. Indeed, upon a second scan, only a minor residual amount is reduced, appearing as a small shoulder at the same potential. In agreement with the CV results, the initial photoelectrochemical performance of the photoelectrodes could be fully restored after potentiostatic conditioning at −400 mV vs SCE for 100 s (Figure S3 in the Supporting Information).

Additional spectroscopic evidence of triiodide adsorption on the TiO_2 photoelectrodes has been obtained by time-resolved laser experiments (Figure S4 in the Supporting Information).

Because adsorption of triiodide at the TiO_2 interface in a aqueous solution was responsible for the observed drop in the photocurrent response, we performed a series of photoelectrochemical experiments using a three-compartment cell configuration where the photoanode was immersed in an NaI/ACN solution, while the counter electrode was immersed in an aqueous acidic solution (1 M HCl).

The $J-V$ characteristics (Figure 12a) recorded under these conditions show the expected behavior of an n-type semiconductor/electrolyte rectifying junction. The photoanodic transients decrease at increasingly negative potentials without the appearance of oscillations in the −300 to −400 mV vs SCE region. Upon subsequent irradiation cycles under a 0 mV vs SCE bias, a photoanodic current of about 5.5 mA/cm^2 was recorded with good stability and reproducibility (Figure 12b). The apparent small decrease of the photocurrent is due to the filtering effect of the yellow I_3^- developing in a few seconds, under such high current densities, in the anodic compartment. The triiodide production was paralleled by evolution of hydrogen at the Pt cathode, resulting in 1.43×10^{-5} mol of H_2 collected in 1190 s, corresponding to an electrolysis yield of 86.6% (Figure 13).[38]

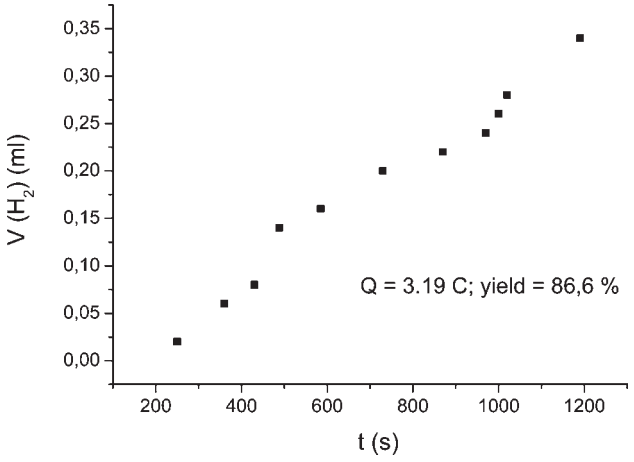

Figure 13. Volume of produced hydrogen as a function of time during the photoelectrolysis employing I^- as a sacrificial electron donor in the cell configuration represented in Scheme 2.

Conclusions

In this preliminary work, we have investigated the possibility of using TiO_2-sensitized photoelectrodes in an aqueous solution containing sacrificial electron donors in order to produce hydrogen. The main goal was to explore the stability

(38) The production and accumulation of I_3^- at the anodic compartment of the cell result in a strong coloration, which limits the light-harvesting efficiency of the photoanode, leading to a slow decrease of the photocurrent, which, for example, in several hundreds of seconds drops to less than 75% of the initial value. Thus, the hydrogen collection time has been limited with respect to the experiment carried out in the presence of ascorbic acid (Figure 9).

of the linkage between the light-absorbing sensitizer and the surface of the wide-band-gap semiconductor as well as the behavior of different hole scavengers in photoelectrosynthetic devices operating under visible-light irradiation at 0 V vs SCE.

A series of ruthenium(II) polypyridine complexes bearing phosphonic acid functional groups at the chromophoric ligands sustained 240 h of irradiation without undergoing appreciable hydrolysis and decomposition in an aqueous environment at pH 3. Despite the demanding kinetics of water oxidation, a reproducible photoanodic response of 5 $\mu A/cm^2$ was detected at pH 5. This fact is relevant and suggests that possible improvements could be obtained by assembling these types of dyes in a polymeric structure favoring concerted multielectron oxidation processes.

As expected, the use of organic sacrificial donors considerably enhanced the photoanodic response, while a common inorganic ion, largely present in nature, such as iodide, was found to limit the efficiency of the photoelectrosynthetic device because of adsorption of the photogenerated I_3^-, which favors charge recombination with conduction band electrons. However, experiments performed in a two-compartment device, where the photoelectrode was in contact with an organic solvent, limiting I_3^- adsorption, showed a remarkable photocurrent, corresponding to 1.5−1 μmol/min/cm^2 of produced hydrogen. This result is comparable to those obtained with the best TiO_2-supported photocatalysts so far reported by other authors.

Acknowledgment. Financial support from ENI Contract R/BGI/19/07 is gratefully acknowledged. We are also thankful for the technical assistance of Sandro Fracasso.

Supporting Information Available: Additional photoelectrochemical and transient spectroscopic measurements. This material is available free of charge via the Internet at http://pubs.acs.org.